Efficient Exciton Harvesting through Long-Range Energy Transfer

Yanbin Wang,[a] Hideo Ohkita,*[a,b] Hiroaki Benten,[a] and Shinzaburo Ito [a]

Efficient exciton collection to charge generation sites is one of the key issues for the improvement in power conversion efficiency (PCE) of organic solar cells because only excitons arriving at a donor/acceptor interface can be dissociated into free charge carriers. We have evaluated the effective diffusion length in poly(3-hexylthiophene) (P3HT) by using donor/acceptor bilayers with two different exciton-quenching acceptors. One is an insoluble fullerene polymer (p-PCBVB), which is an efficient electron-accepting material with negligible absorption in the visible region. The other is a low-bandgap polymer, poly[(4,4-bis(2-ethylhexyl)-dithieno[3,2-b:2',3'-d]silole)-2,6-diyl-*alt*-(2,1,3-benzothiadiazole)-4,7-diyl], (PSBTBT). This polymer has a large absorption band in the near-IR region, which is well overlapped with the emission band of P3HT. The effective diffusion length of P3HT excitons is evaluated to be 15 nm for P3HT/p-PCBVB bilayers and improved to 30 nm for P3HT/PSBTBT bilayers. This improvement is ascribed to long-range energy transfer from P3HT to PSBTBT. This finding suggests that effective diffusion length of P3HT excitons can be increased through long-range energy transfer by incorporating PSBTBT to P3HT/PCBM blends.
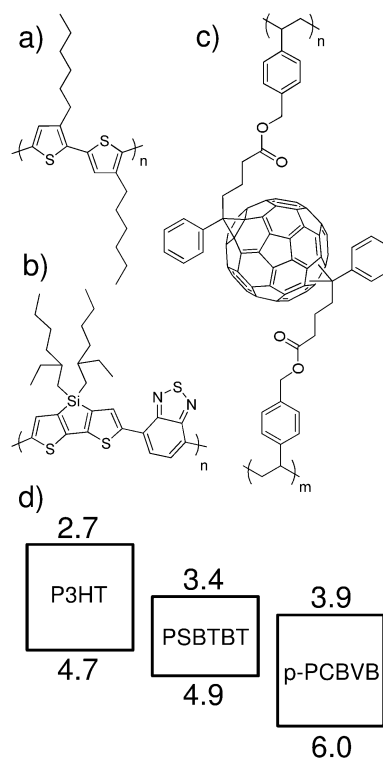
1. Introduction

Polymer solar cells have attracted a great deal of attention because of their potential applications to flexible, light-weight, and large-area devices.[1–3] The active layer of them is typically based on bulk heterojunction structures, which consist of donor and acceptor materials with interpenetrating nanoscale networks to maximize the donor/acceptor interfacial area. In polymer solar cells, excitons (coulombically bound electron–hole pairs) should be transferred to the donor/acceptor interface to be efficiently dissociated into free electron and hole carriers because of the strong binding energy.[4–6] However, the exciton diffusion length in most conjugated polymers is as short as 5–20 nm,[7–15] which is not always enough to make sure all the excitons generated reach the interface of polymer/fullerene before deactivating to the ground state. For example, it has been reported that about 10–20% excitons are lost before arriving at the interface even in a benchmark solar cell based on poly(3-hexylthiophene) (P3HT) and a fullerene derivative (PCBM).[16,17] Therefore, the efficient exciton harvesting is required for further improvement in polymer solar cells.

Energy transfer is long-range exciton transport and hence could collect exciton energy more efficiently to specific sites than random exciton diffusion if energy donating and accepting materials are allocated appropriately.[17–21] Indeed, we have recently shown that P3HT excitons are collected more efficiently to a low-bandgap dye molecule silicon phthalocyanine derivative (SiPc) located at a donor/acceptor interface in P3HT/PCBM blends.[17,21–23] As a result of such appropriate incorporation of SiPc, the external quantum efficiency (EQE) is improved not only at the dye absorption band in the near-IR region but also at the P3HT absorption band in the visible region. The former is ascribed to the additional light-harvesting by SiPc dye molecules. The latter is ascribed to long-range energy transfer from P3HT

to SiPc at the heterojunction of P3HT/PCBM blends. Because of the spectral overlap between P3HT emission and SiPc absorption bands, the Förster radius is as long as 3.7 nm, which is enough long compared to a hopping length of excitons. In P3HT/PCBM/SiPc ternary blends, half of P3HT excitons that would be lost in the absence of SiPc are collected by energy transfer to SiPc molecules at the heterojunction. Consequently, our finding demonstrates that the energy transfer can increase the effective exciton diffusion length.

Recently, the photocurrent improvement has been reported for ternary blend solar cells based on P3HT, PCBM, and a low-

Scheme 1. Chemical structures of materials used in this study: a) P3HT, b) PSBTBT, and c) p-PCBVB. d) The HOMO (lower) and LUMO (upper) energy levels of these materials.

[a] Dr. Y. Wang, Dr. H. Ohkita, Dr. H. Benten, Prof. S. Ito,
Department of Polymer Chemistry, Graduate School of Engineering,
Kyoto University, Katsura, Nishikyo, Kyoto 615-8510, Japan
E-mail: ohkita@photo.polym.kyoto-u.ac.jp

[b] Dr. H. Ohkita
Japan Science and Technology Agency (JST), PRESTO, 4-1-8
Honcho Kawaguchi, Saitama 332-0012, Japan

bandgap polymer PSBTBT.[24–28] This was primarily ascribed to the additional light-harvesting in the near-IR region due to PSBTBT. We speculate that the energy transfer from P3HT to PSBTBT would improve the exciton harvesting and hence the device performance in this ternary blend solar cells because of the spectral overlap between P3HT emission and PSBTBT absorption bands. Herein, we study the effective diffusion length of P3HT excitons to PSBTBT domains in order to address how energy transfer impacts on the diffusion length in P3HT/PSBTBT/PCBM ternary blends. To evaluate the exciton diffusion length of P3HT excitons correctly, we employed bilayer films based on P3HT and insoluble fullerene polymer (p-PCBVB). In these polymer/fullerene bilayers, P3HT excitons would be quenched dominantly by electron transfer at the interface. On the other hand, the effective diffusion length of P3HT excitons was evaluated for P3HT/PSBTBT bilayers in comparison with that in P3HT/p-PCBVB bilayers. In these polymer/polymer bilayers, P3HT excitons would be quenched dominantly by energy transfer to the interface.

2. Theory

The continuity equation of the exciton density in one-dimensional diffusion is given by Equation (1)

$$\frac{\partial n(x,t)}{\partial t} = D\frac{\partial^2 n(x,t)}{\partial x^2} - \frac{n(x,t)}{\tau} + G(x) \tag{1}$$

where $n(x,t)$ is the exciton density at a position x and time t, D is the exciton diffusion coefficient, τ is the exciton lifetime without quenching wall, and $G(x)$ is the exciton generation rate at a position x. Under steady state condition, this equation can be solved with two boundary conditions at the two interfaces [Eqs. (2) and (3)].

$$n(L,t) = 0 \tag{2}$$

$$D\frac{\partial n(x,t)}{\partial x}\bigg|_{x=0} = 0 \tag{3}$$

In Equation (2), it is assumed that all the excitons arriving at the interface $x = L$ are quenched with 100% efficiency. In Equation (3), it is assumed that the excitons arriving at the air/polymer interface $x = 0$ are not quenched at all and just reflected. In this manner, an analytical expression for the exciton quenching efficiency $Q(L)$ is given by Equation (4) as a function of the polymer film thickness L

$$Q(L)$$
$$= \frac{\left[\alpha^2 L_D^2 + \alpha L_D \tanh\left(\frac{L}{L_D}\right)\right]\exp(-\alpha L) - \alpha^2 L_D^2\left[\cosh\left(\frac{L}{L_D}\right)\right]^{-1}}{(1 - \alpha^2 L_D^2)[1 - \exp(-\alpha L)]} \tag{4}$$

where α as the absorption coefficient of the donor material and the exciton diffusion length $L_D = \sqrt{D\tau}$.

When excitons are quenched not only by electron transfer at the interface but also by long-range energy transfer to the interface $x = L$, an additional quenching term should be added to

Equation (1). This is true for low-bandgap acceptors such as PSBTBT. In this case, an additional quenching term is added as shown in Equation (5).[19]

$$\frac{\partial n(x,t)}{\partial t} = D\frac{\partial^2 n(x,t)}{\partial x^2} - \frac{n(x,t)}{\tau} - k_{\mathrm{EnT}}(x)n(x,t) + G(x) \tag{5}$$

Here, $k_{\mathrm{EnT}}(x)$ is the energy transfer rate from position x to the interface $x = L$, which is given by Equation (6)

$$k_{\mathrm{EnT}}(x) = \frac{C_A}{\tau}\frac{\pi}{6}\frac{R_0^6}{(L - x)^3} \tag{6}$$

where C_A is the density of energy-accepting molecules, and R_0 is the Förster radius. McGehee et al. reported that the exciton diffusion length effectively increases in the presence of the energy transfer mechanism. Interestingly, they also found that the exciton quenching data in the presence of the energy transfer can be still well reproduced by Equation (4) even though only exciton diffusion is considered.[20] For comparison, we therefore evaluate the effective diffusion length by Equation (4) for the exciton quenching in the absence and presence of long-range energy transfer.

3. Results and Discussion
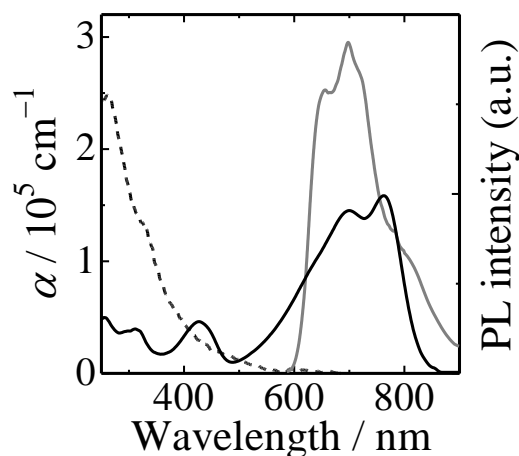
3.1. Optoelectronic Properties

Figure 1. Absorption spectra of PSBTBT (black solid line) and p-PCBVB (black broken line) and PL spectrum of P3HT (gray line) neat films.

The highest occupied molecular orbital (HOMO) level was estimated to be 4.7 eV for P3HT, 4.9 eV for PSBTBT, and 6.0 eV for p-PCBVB in the solid state by photoemission yield spectroscopy. The lowest unoccupied molecular orbital (LUMO) level was evaluated to be 2.7 eV for P3HT, 3.4 eV for PSBTBT, and 3.9 eV for p-PCBVB from the HOMO level and the optical bandgap estimated from the absorption and emission spectra. As shown in Scheme 1d, these energy structures make sure efficient charge separation between P3HT and p-PCBVB and between P3HT and PSBTBT. As shown in Figure 1, the fullerene polymer p-PCBVB exhibits large absorption in the

ultraviolet region but negligible absorption in the visible region and the low-bandgap PSBTBT exhibits a large absorption band at around 700 nm with an absorption coefficient of 145 000 cm^{-1}. On the other hand, as shown in the figure, P3HT exhibits an emission band at around 700 nm, which negligibly overlapped with the absorption of p-PCBVB but well overlapped with the absorption band of PSBTBT. From the spectral overlap between the absorption and emission band, the Förster radius is estimated to be as short as 1.6 nm for the energy transfer from P3HT to p-PCBVB but as long as 3.5 nm for the energy transfer from P3HT to PSBTBT. These optoelectronic properties indicate that P3HT excitons are quenched by electron transfer at the interface with p-PCBVB or PSBTBT and also quenched by long-range energy transfer to the interface of PSBTBT.
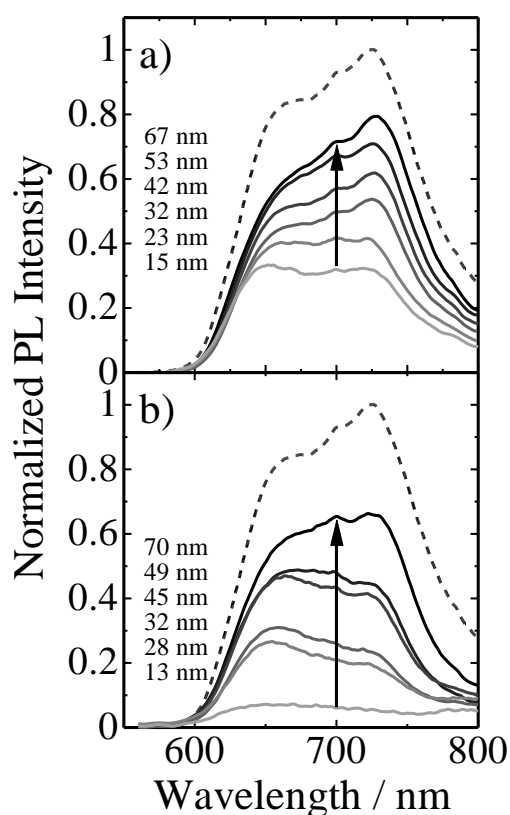
3.2. Exciton Diffusion Length

Figure 2. PL spectra of a) P3HT/p-PCBVB and b) P3HT/PSBTBT bilayer films with different P3HT thickness. The broken lines represent the PL spectra of P3HT neat films. The PL intensity of each bilayer film was normalized by the intensity of P3HT neat films with the same thickness.

In order to accurately evaluate the exciton diffusion length, we employ an insoluble fullerene polymer p-PCBVB as an electron-accepting layer in donor/acceptor bilayers instead of small molecule acceptors such as a fullerene derivative PCBM. As reported recently, PCBM molecules are likely to diffuse into the other layer in bilayers even at room temperature.[29] On the other hand, as we reported previously, p-PCBVB insoluble films exhibit flat and smooth surface, which can serve as a suitable quenching wall in donor/acceptor bilayers for evaluating the

exciton diffusion length.[9] The thickness of P3HT layers was varied from 10 to 70 nm, which was precisely evaluated with an absorption coefficient of P3HT. For all the films employed in this study, P3HT was selectively excited in nitrogen atmosphere to prevent PL quenching at the P3HT/air surface.

For P3HT/p-PCBVB bilayers, as shown in Figure 2a, the normalized PL intensity of P3HT decreased with decreasing P3HT thickness. This is because most P3HT excitons can diffuse to the P3HT/p-PCBVB interface in the thinner P3HT layer and hence are quenched efficiently. For P3HT/PSBTBT bilayers, as shown in Figure 2b, the normalized PL intensity of P3HT more steeply decreased with decreasing P3HT thickness than that for P3HT/p-PCBVB. Instead, as shown in Figure 3, the PL band of PSBTBT was observed even though P3HT was selectively excited at 485 nm. The PL intensity due to direct excitation of PSBTBT was negligibly small as shown in the figure: it was as small as 5% at most because the PSBTBT absorption is the smallest at 485 nm. Thus, the PSBTBT emission observed is indicative of energy transfer from P3HT to PSBTBT.
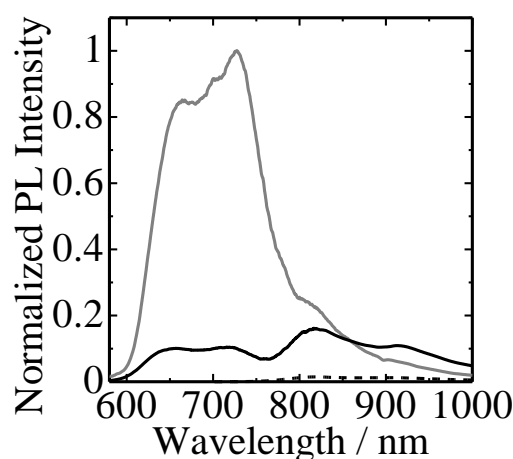

Figure 3. PL spectra of P3HT/PSBTBT bilayer (black line), P3HT neat (gray line), and PSBTBT neat (broken line) films excited at 485 nm. The thickness of each layer was 14 nm (P3HT) and 20 nm (PSBTBT).

Figure 4 shows the quenching efficiency of P3HT in the two bilayer models plotted against the P3HT thickness. The solid lines represent theoretical curves calculated by Equation (4) with various diffusion lengths. For P3HT/p-PCBVB bilayers, as shown in Figure 4a, the quenching efficiency is well fitted with a diffusion length of 15 nm, which is slightly shorter than that in P3HT crystalline domains recently reported (20 nm).[10] This is probably because the diffusion length evaluated for the bilayer is average of exciton diffusions in amorphous and crystalline domains. For P3HT/PSBTBT bilayers, as shown in Figure 4b, the quenching efficiency is well fitted with an effective diffusion length of 30 nm, which is two times longer than that for P3HT/p-PCBVB bilayers. This is because P3HT excitons are more

effectively collected to the PSBTBT quenching wall by efficient energy transfer.
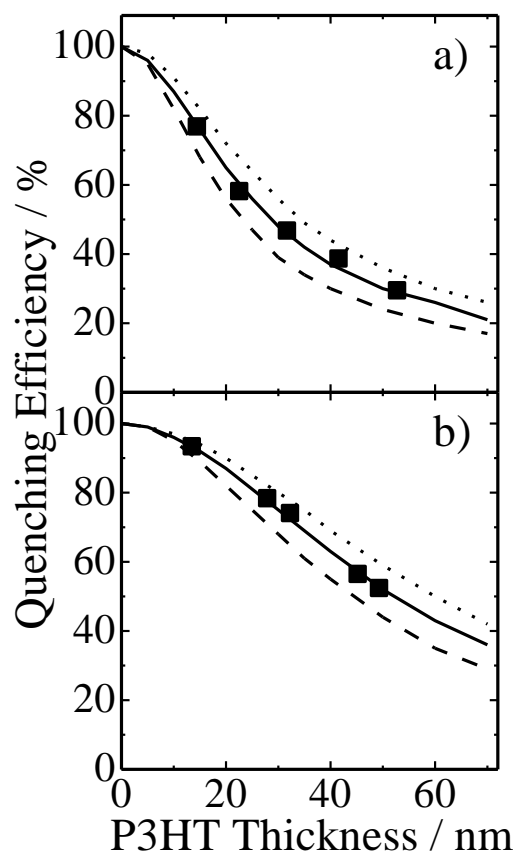

Figure 4. PL quenching efficiency of a) P3HT/p-PCBVB and b) P3HT/PSBTBT bilayer films plotted against P3HT thickness. The broken, solid, and dotted lines represent the PL quenching efficiency calculated by Equation 4 with an exciton diffusion length of 12, 15, and 18 nm (panel a) and 25, 30, and 35 nm (panel b), respectively.

Finally, we note the relevance of the effective diffusion length to photovoltaic performance of ternary blend solar cells. More specifically, we focus on ternary solar cells based on P3HT, PSBTBT, and PCBM. In this blend, P3HT is the most crystalline material and hence would form large crystalline domains under appropriate fabrication conditions such as thermal or solvent annealing. Consequently, PSBTBT also would form phase-separated domains, which are probably mixed with PCBM as reported previously.[30,31] Typically, phase-separated domain size would be of the order of tens of nanometers, which is consistent with the acceptor thickness employed in this study. We therefore propose that energy transfer from P3HT to PSBTBT would be efficient in ternary blends with large P3HT crystalline domains. In other words, the energy transfer can harvest more efficiently P3HT excitons that would be lost in such large crystalline domains in the absence of PSBTBT. The large P3HT crystalline domains would be beneficial for the efficient charge transport and hence improve photovoltaic performance.

4. Conclusions

In summary, we demonstrated that the effective diffusion length of singlet excitons can be increased by long-range energy transfer. In P3HT/p-PCBVB bilayer films, the diffusion length of P3HT excitons is evaluated to be 15 nm, which is slightly shorter than that evaluated for P3HT crystalline domains by singlet exciton–exciton annihilation. In other words, this exciton diffusion length is an average value for P3HT amorphous and crystalline domains. In P3HT/PSBTBT bilayer films, on the other hand, the effective diffusion length of P3HT excitons is evaluated to be 30 nm. This is most probably because P3HT excitons are more efficiently collected to the PSBTBT quenching wall in the bilayer film. The Förster radius is estimated to be 3.5 nm for the energy transfer from P3HT to PSBTBT on the basis of the spectral overlap. In ternary blends of P3HT, PSBTBT, and PCBM, the energy transfer would enhance the effective diffusion length as is the case with the bilayer system employed in this study. We therefore propose that growing large P3HT crystalline domains would be the key to the improvement in photovoltaic performance of P3HT/PSBTBT/PCBM ternary solar cells.

Experimental Section

Materials

A cross-linkable bi-functionalized fullerene derivative (bis-PCBVB) was synthesized according to literatures.[32,33] The insoluble fullerene polymer p-PCBVB was obtained by thermal cross-linking of bis-PCBVB at 170 °C for 1 h. The details have been described elsewhere.[9] The other chemicals were used without any purification unless otherwise noted: P3HT (Sigma–Aldrich, regioregular, M_n = 87,000 g mol^{-1}) and PSBTBT (Solarmer Materials Inc., M_n =11,900 g mol^{-1}). The chemical structures and energy levels of materials used in this study are summarized in Scheme 1.

Fabrication of Bilayers

Bilayer films of P3HT/p-PCBVB were fabricated as follows. First, bis-PCBVB layer was spin-coated on quartz substrates from chlorobenzene solution (4 mg mL^{-1}) at a spin rate of 1000 rpm for 60 s. Prior to the spin-coating, the quartz substrates were washed by ultrasonication in toluene, acetone, and ethanol for 15 min in sequence, dried with nitrogen gas, and then cleaned with UV–ozone cleaner for 30 min. Subsequently, the bis-PCBVB film was thermally annealed at 170 °C for 1 h under nitrogen atmosphere to be converted to cross-linked and insoluble p-PCBVB film. The p-PCBVB film was rinsed with chlorobenzene twice and dried for next step. On the other hand, polymer layers were separately prepared on glass substrates by successive spin-coatings of poly(sodium 4-styrenesulfonate) (PSS: Sigma–Aldrich, M_w = 70,000 g mol^{-1}) and P3HT, resulting in a layered structure with glass/PSS/P3HT. Here, PSS was employed as a sacrificial layer and prepared by spin-coating on pre-cleaned glass substrates from an aqueous solution of PSS (10 mg mL^{-1}) at a spin rate of at 400 rpm for 10 s and 4000 rpm for 30 s. By immersing the glass substrate coated with PSS/P3HT into water slowly, the P3HT layer was floated on the water because the PSS sacrificial layer was selectively dissolved. Finally, the quartz substrate coated with p-PCBVB was gently placed on the P3HT film to obtain a bilayer film of P3HT/p-PCBVB.

Bilayer films of P3HT/PSBTBT were fabricated in a similar fashion. First, PSBTBT layer was prepared by spin-coating on the cleaned quartz

substrate from a chlorobenzene solution with a concentration of 4 mg mL^{-1} at a spin rate of 2000 rpm for 60 s. Subsequently, a P3HT layer was transferred from the water surface to the PSBTBT coated substrate as is the case with P3HT/p-PCBVB bilayers.

Measurements

Absorption and photoluminescence (PL) spectra were measured with a spectrophotometer (Hitachi, U-3500) and a spectrofluorometer (Horiba Jobin Yvon, NanoLog) equipped with a calibrated imaging detector (Horiba Jobin Yvon, iHR320), respectively. The optical bandgap of materials used in this study was evaluated from the wavelength of intersection between the absorption and PL spectra. The film thickness was evaluated with an atomic force microscope (Shimadzu, SPM-9500J) in the contact mode at room temperature. The ionization potential of P3HT, PSBTBT, and p-PCBVB was measured with a photoelectron yield spectrometer (Riken Keiki, AC-3). All the neat films (ca. 60 nm) were fabricated by spin-coating from each chlorobenzene solution on the ITO substrate. The threshold energy for the photoelectron emission was estimated on the basis of the cubic root of the photoelectron yield plotted against the incident photon energy.
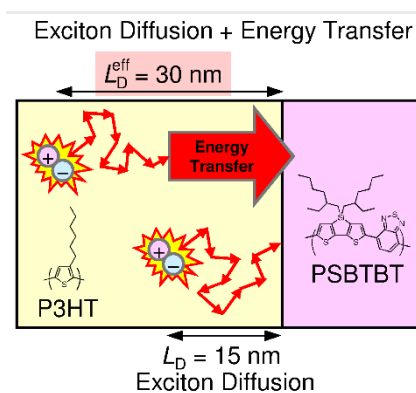
Acknowledgements

[1] M. C. Scharber, N. S. Sariciftci, *Prog. Polym. Sci.* **2013**, *38*, 1929–1940.

[2] N. Yeh, P. Yeh, *Renew. Sust. Energy Rev.* **2013**, *21*, 421–431.

[3] L. Dou, J. You, Z. Hong, Z. Xu, G. Li, R. A. Street, Y. Yang, *Adv. Mater.* **2013**, *25*, 6642–6671.

[4] C. Deibel, V. Dyakonov, *Rep. Prog. Phys.* **2010**, *73*, 096401.

[5] H. Ohkita, S. Ito, *Polymer* **2011**, *52*, 4397–4417.

[6] P. Peumans, A. Yakimov, S. R. Forrest, *J. Appl. Phys.* **2003**, *93*, 3693–3723.

[7] S. M. Menke, R. J. Holmes, *Energy Environ. Sci.* **2014**, *7*, 499–512.

[8] C. Leow, T. Ohnishi, M. Matsumura, *J. Phys. Chem. C* **2014**, *118*, 71–76.

[9] Y. Wang, H. Benten, S. Ohara, D. Kawamura, H. Ohkita, S. Ito, *ACS Appl. Mater. Interfaces* **2014**, *6*, 14108–14115.

[10] Y. Tamai, Y. Matsuura, H. Ohkita, H. Benten, S. Ito, *J. Phys. Chem. Lett.* **2014**, *5*, 399–403.

[11] O. V. Mikhnenko, H. Azimi, M. Scharber, M. Morana, P. W. M. Blom, M. A. Loi, *Energy Environ. Sci.* **2012**, *5*, 6960–6965.

[12] K. Masuda, Y. Ikeda, M. Ogawa, H. Benten, H. Ohkita, S. Ito, *ACS Appl. Mater. Interfaces* **2010**, *2*, 236–245.

[13] A. J. Lewis, A. Ruseckas, O. P. M. Gaudin, G. R. Webster, P. L. Burn, I. D. W. Samuel, *Org. Electron.* **2006**, *7*, 452–456.

[14] P. E. Shaw, A. Ruseckas, I. D. W. Samuel, *Adv. Mater.* **2008**, *20*, 3516–3520.

[15] D. E. Markov, E. Amsterdam, P. W. M. Blom, A. B. Sieval, J. C. Hummelen, *J. Phys. Chem. A* **2005**, *109*, 5266–5274.

[16] A. L. Ayzner, D. D. Wanger, C. J. Tassone, S. H. Tolbert, B. J. Schwartz, *J. Phys. Chem. C* **2008**, *112*, 18711–18716.

[17] S. Honda, T. Nogami, H. Ohkita, H. Benten, S. Ito, *ACS Appl. Mater. Interfaces* **2009**, *4*, 804–810.

[18] Y. Liu, M. A. Summers, C. Edder, J. M. J. Frechet, M. D. McGehee, *Adv. Mater.* **2005**, *17*, 2960–2964.

[19] S. R. Scully, M. D. McGehee, *J. Appl. Phys.* **2006**, *100*, 034907.

[20] S. R. Scully, P. B. Armstrong, C. Edder, J. M. J. Frechet, M. D. McGehee, *Adv. Mater.* **2007**, *19*, 2961–2966.

[21] S. Honda, S. Yokoya, H. Ohkita, H. Benten, S. Ito, *J. Phys. Chem. C* **2011**, *115*, 11306–11317.

[22] S. Honda, H. Ohkita, H. Benten, S. Ito, *Chem. Commun.* **2010**, *46*, 6596–6598.

[23] S. Honda, H. Ohkita, H. Benten, S. Ito, *Adv. Energy Mater.* **2011**, *1*, 588–598.

[24] T. Ameri, J. Min, N. Li, F. Machui, D. Baran, M. Forster, K. J. Schottler, D. Dolfen, U. Scherf, C. J. Brabec, *Adv. Energy Mater.* **2012**, *2*, 1198–1202.

[25] T. Ameri, T. Heumuller, J. Min, N. Li, G. Matt, U. Scherf, C. J. Brabec, *Energy Environ. Sci.* **2013**, *6*, 1796–1801.

[26] M. Koppe, H. J. Egelhaaf, E. Clodic, M. Morana, L. Luer, A. Troeger, V. Sgobba, D. M. Guldi, T. Ameri, C. J. Brabec, *Adv. Energy Mater.* **2013**, *3*, 949–958.

[27] N. Li, F. Machui, D. Waller, M. Koppe, C. J. Brabec, *Sol. Energy Mater. Sol. Cells* **2011**, *95*, 3465–3471.

[28] F. Machui, S. Rathgeber, N. Li, T. America, C. J. Brabec, *J. Mater. Chem.* **2012**, *22*, 15570–15577.

[29] N. D. Treat, T. E. Mates, C. J. Hawker, E. J. Kramer, M. L. Chabinyc, *Macromolecules* **2013**, *46*, 1002–1007.

[30] M. T. Dang, L. Hirsch, G. Wantz, J. D. Wuest, *Chem. Rev.* **2013**, *113*, 3734–3765.

[31] H. Y. Chen, J. Hou, A. E. Hayden, H. Yang, K. N. Houk, Y. Yang, *Adv. Mater.* **2010**, *22*, 371–375.

[32] B. Kim, H. R. Yeom, W. Y. Choi, J. Y. Kim, C. Yang, *Tetrahedron* **2012**, *68*, 6696–6700.

[33] C. H. Hsieh, Y. J. Cheng, P. J. Li, C. H. Chen, M. Dubosc, R. M. Liang, C. S. Hsu, *J. Am. Chem. Soc.* **2010**, *132*, 4887–4893.

Entry for the Table of Contents (Please choose one layout)

ARTICLE

Efficient exciton harvesting: Effective diffusion length of P3HT excitons can be doubled from 15 nm to 30 nm in bilayers of a wide-bandgap polymer P3HT and a low-bandgap polymer PSBTBT. This is mainly due to long-range energy transfer from P3HT excitons to PSBTBT because of large spectral overlap between P3HT emission and PSBTBT absorption band.

Exciton Diffusion + Energy Transfer
L_D^{eff} = 30 nm
Energy Transfer
P3HT
PSBTBT
L_D = 15 nm
Exciton Diffusion

Y. Wang, H. Ohkita, H. Benten, S. Ito*

Page No. – Page No.

Efficient Exciton Harvesting through Long-Range Energy Transfer